NASA CR-180792

EFFECTS OF SWITCH LEAKAGES UPON NIMBUS-7 SMMR CALIBRATION

Daesoo Han
NASA Goddard Space Flight Center
Greenbelt, Maryland

Seung T. Kim
ST Systems Corporation
9701 J Philadelphia Way
Lanham, Maryland

June 1988

GODDARD SPACE FLIGHT CENTER
Greenbelt, Maryland

TABLE OF CONTENTS

1.0 INTRODUCTION

The Nimbus-7 Scanning Multichannel Microwave Radiometer (SMMR) consists of six conventional Dicke-type radiometers: two, operating at 37 GHz, measuring simultaneously the horizontal and vertical polarizations; the other four, operating at 6.6, 10.7, 18, and 21 GHz, measuring the two orthogonal polarizations alternately during a scan. Thus the SMMR provides ten data channels, corresponding to two orthogonal polarizations at five frequencies. A description of the SMMR instrument was given by Gloersen and Barath (1977). Only those instrument characteristics that sre relevant to this study will be pointed out in this and later sections.

All six radiometers share a single offset parabolic reflector. While the reflector scans 25° to the left and right of the satellite flight direction, the multi-frequency feed horn (MFFH) remains fixed. This configuration of the fixed MFFH relative to the scanning reflector introduces a polarization mixing in the measured signal, which would be given by Eq. (1) below, if the instrument were perfect:

$$\begin{pmatrix} T_x \\ T_y \end{pmatrix} = \begin{pmatrix} \cos^2\phi & \sin^2\phi \\ \sin^2\phi & \cos^2\phi \end{pmatrix} \begin{pmatrix} H \\ V \end{pmatrix}, \tag{1}$$

where T_x and T_y are measured radiances for horizontal and vertical channels, respectively, H and V are horizontal and vertical components of the surface radiance, respectively, and ϕ is the scan angle. In Eq. (1), T_x and T_y are symmetric about the scan angle $\phi=0$. However, as noticed by Gloersen et al. (1980) and Gloersen (1983), the measured radiances are not symmetric about scan angle $\phi=0$, but the whole shape is shifted as shown in Fig. 1. The cause of the shift was not well understood at that time. So, to compensate for the shift, "offset angles", δ_x and δ_y were empirically introduced in the following manner:

$$\begin{pmatrix} T_x \\ T_y \end{pmatrix} = \begin{pmatrix} \cos^2(\phi + \delta_x) & \sin^2(\phi + \delta_x) \\ \sin^2(\phi + \delta_y) & \cos^2(\phi + \delta_y) \end{pmatrix} \begin{pmatrix} H \\ V \end{pmatrix}, \tag{2}$$

where the values of δ_x and δ_y are determined from the measured data using regression technique.

The radiometers operating at lower four frequencies utilize polarization selector switches for measuring one of the two polarizations. There are leakages in a polarization selector switch, which is about 1 % of the total input power. In Section 2.1, it is shown that the leakages, though small, cause interference between the signal to be measured and the one to be suppressed, thus generating a term which is not symmetric about $\phi=0$. There is also additional mixing between the two polarizations that arises from the leakages at other switches. The same procedure is followed in Section 2.2 to derive a new set of calibration equations for the 37 GHz radiometers which do not need a polarization selector switch.
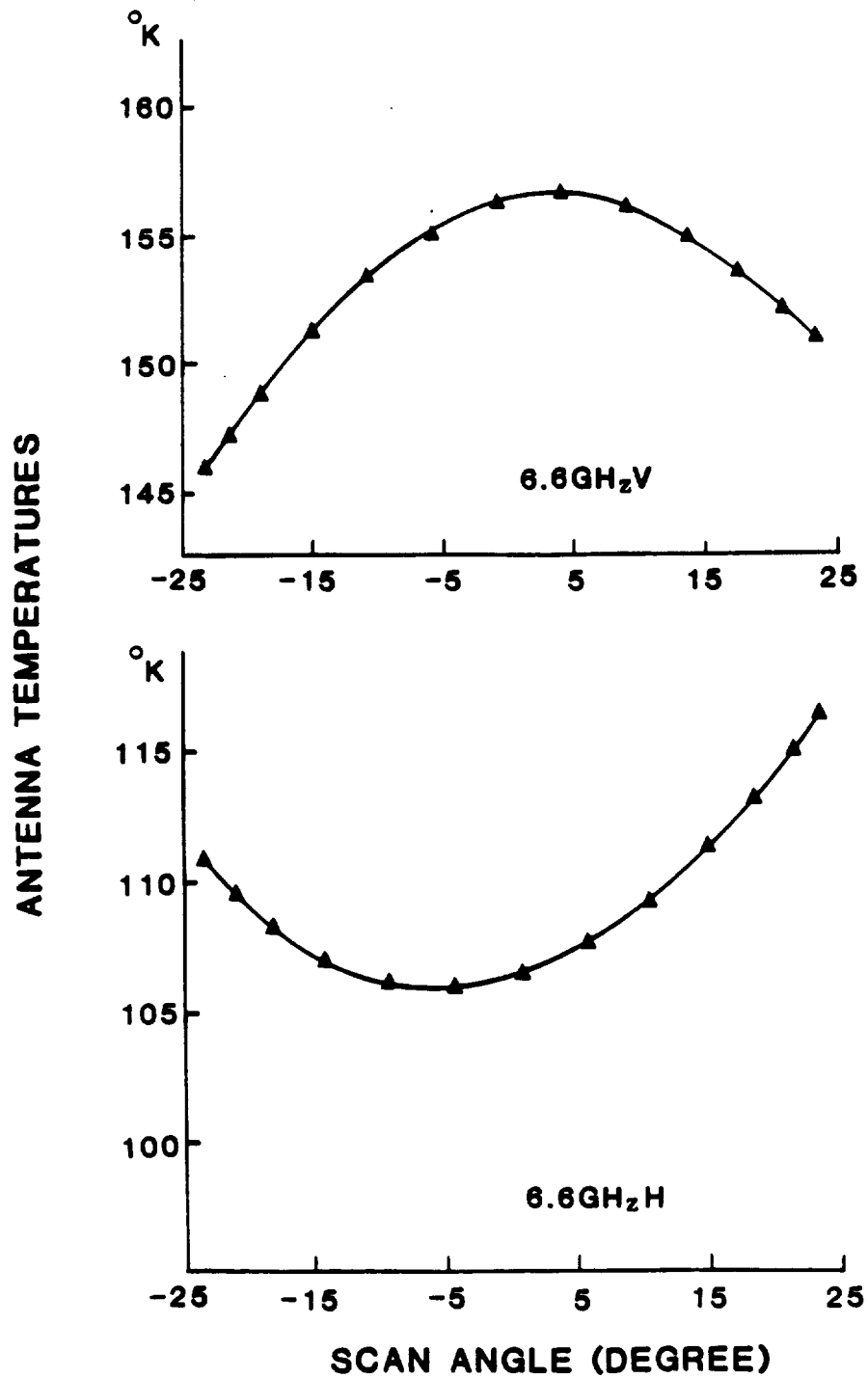
1

FIGURE 1. Averaged antenna temperatutes for 6.6 GHz horizontal and verticalchannels versus scan angle. For averaging, one month of November, 1978 data over Pacific ocean are used.

In Section 3, it is shown that the current calibration equations can be derived from the new ones if switch leakages are ignored. In the last section, methods to analyze in-flight data to obtain "absolutely calibrated" radiances are briefly discussed.

2.0 CALIBRATION EQUATIONS

The basic calibration scheme of the SMMR utilizes a two-point reference signal system consisting of an ambient RF termination and a horn antenna viewing deep space with known brightness temperatures. However the situation gets complicated because the ferrite switches that selects particular signal paths have non-negligible leakages. The measured radiances of the cold reference targets have additional leakage-dependent components that are different from those form the warm reference targets. These leakage-induced biases are also different from those coming from the paths chosen for measuring the surface radiances. Therfore it is necessary to treat individual signal paths separately to identify and compensate for the leakage-dependent bias terms.

In Subsection 2.1, a set of new calibration equations are derived for the the radiometers operating at lower four frequencies that utilize ferrite switches to select one of the two orthogonally polarized radiances. Separate treatment is provided in Subsection 2.2 for the two radiometers operating at 37 GHz - one for each of the two orthogonal polarizations.

2.1 Channels with a polarization selector switch

A schematic diagram of the RF components for a typical radiometer, which provides two orthogonal polarization channels operating at a common frequency, is shown in Fig. 2. In addition to the familiar modulator (or Dicke) switch, there are three latching ferrite switches: the sky/ambient switch (c) which selects a signal from either a sky horn or an ambient load; the polarization selector switch (p) which selects either a horizontally or vertically polarized signal from the multi-frequency feed horn; the cal/sig switch (s) which selects a signal from either switch c or p. These three switches, when suitably set, provide four distinct signal paths to the modulator switch input port marked I in Fig. 2; two paths for cold and warm reference signals and another two paths for horizontally and vertically polarized radiances.

In the following we will derive a relationship between the target temperature and the power at port I by piecing together the input-output relationships for individual RF components along each signal path. By way of introducing notations, we write down generic input-output relationships for two- and three-port devices. For a two-port device, (with input port A and output port B, as shown in Fig. 3), the output power, T_B is given by

$$T_B = \alpha T_A + (1-\alpha)t, \tag{3}$$

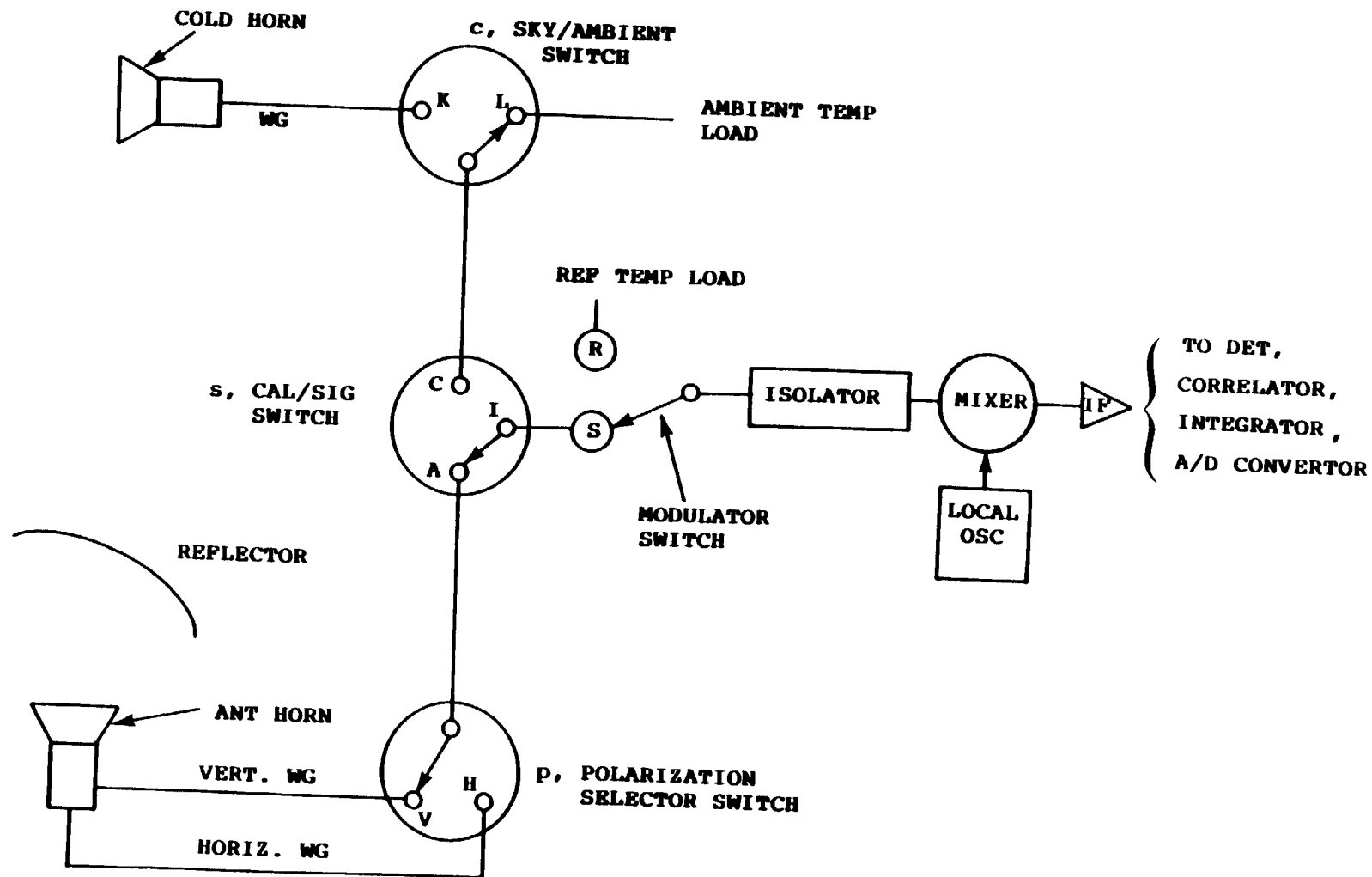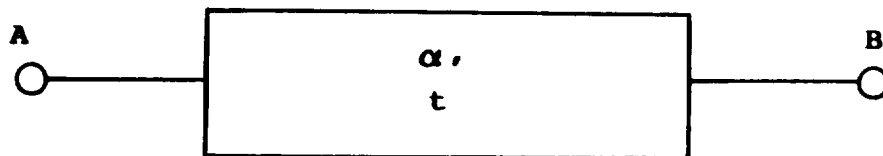where T_A is the input power, α is the transmissivity of the device,

FIGURE 2. Schematic diagram of RF components of the Nimbus-7 SMMR.
- except for the 37 Ghz channels.

$T_B = \alpha T_A + (1-\alpha)\, t,$

T_A = POWER AT INPUT PORT A

T_B = POWER AT OUTPUT PORT B

α = TRANSMISSIVITY

t = PHYSICAL TEMPERATURE

FIGURE 3. Input-output relationship for a two-port device.

and t is the physical temperature . For a ferrite switch x (=p,c,s) with input ports A and B and output port C, the output power, T_C, when port A is selected (see Fig. 4), is assumed to be given by

$$T_C = \alpha_{xAC}T_A + \beta_{xBC}T_B + (1-\alpha_{xAC})t, \tag{4}$$

where T_A and T_B are input powers at ports A and B, respectively, α_{xAC} is the transmissivity from A to C, β_{xBC} is the leakage factor from B to C, and t is the device's physical temperature.

We start with microwave radiation emitted from the earth's surface, which may be expressed in terms of electric field as

$$E = \begin{pmatrix} E_x \exp(iwt) \\ E_y \exp(iwt + i\Omega) \end{pmatrix}, \tag{5}$$

where E_x and E_y are the horizontal and vertical components of the electric field defined on the coordinate system connecting the earth surface and the antenna (Fig. 5), w is the microwave frequency, and Ω is the phase difference which is assumed to have any value between 0 and 2π with equal probability. The electric field, E is reflected by the reflector to the feed horn. Since the feed horn coordinates are rotated relative to the scanning reflector by an amount of scan angle ϕ, the two orthogonal components E_{1x} and E_{1y} selected by the horn are given by

$$E_1 = \begin{pmatrix} \cos \phi & \sin \phi \\ -\sin \phi & \cos \phi \end{pmatrix} E. \tag{6}$$

The two orthogonal components are routed separately to switch p via waveguides or coaxial cables, undergoing attenuation by a factor of g_x and g_y, respectively. Though prelaunch test results suggested that the switch leakages from an unselected input port to the output port should be negligible, the effective leakages may not be negligible, when mismatched components are attached to the ports. We denote by k_{1x} the magnitude of the blocked portion of the horizontal polarization component, and by k_{2x} the leaked portion from the vertical polarization added to the horizontal component; and similarly for k_{1y} and k_{2y}. We note that these quantities are related to the transmissivities and leakage factors of switch p as follows:
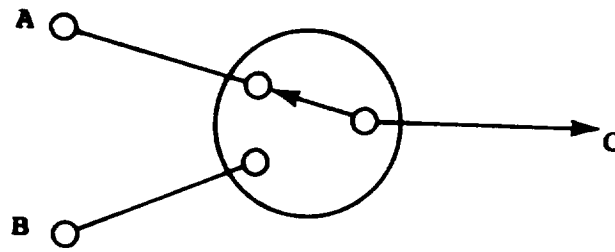
$$\alpha_{pHA} = (1 - k_{1x})^2,$$

$$\alpha_{pVA} = (1 - k_{1y})^2,$$

$$\beta_{pHA} = k_{2y}^2,$$

$$\beta_{pVA} = k_{2x}^2.$$

Immediately after a polarization is selected, the electric field, E_2 would be given by

6

$$\alpha_{AC}, \ \alpha_{BC}$$
$$\beta_{AC}, \ \beta_{BC}$$

$$T_C = \alpha_{AC} \ T_A + \beta_{BC} \ T_B + (1 - \alpha_{AC}) \ t,$$

$$T_A, \ T_B = \text{POWERS AT INPUT PORTS A AND B, RESP.}$$

$$T_C = \text{POWER AT OUTPUT PORT C}$$

$$\alpha_{A_1 A_2} = \text{TRANSMISSIVITY FROM } A_1 \text{ TO } A_2$$

$$\beta_{A_1 A_2} = \text{LEAKAGE FACTOR FROM } A_1 \text{ TO } A_2$$

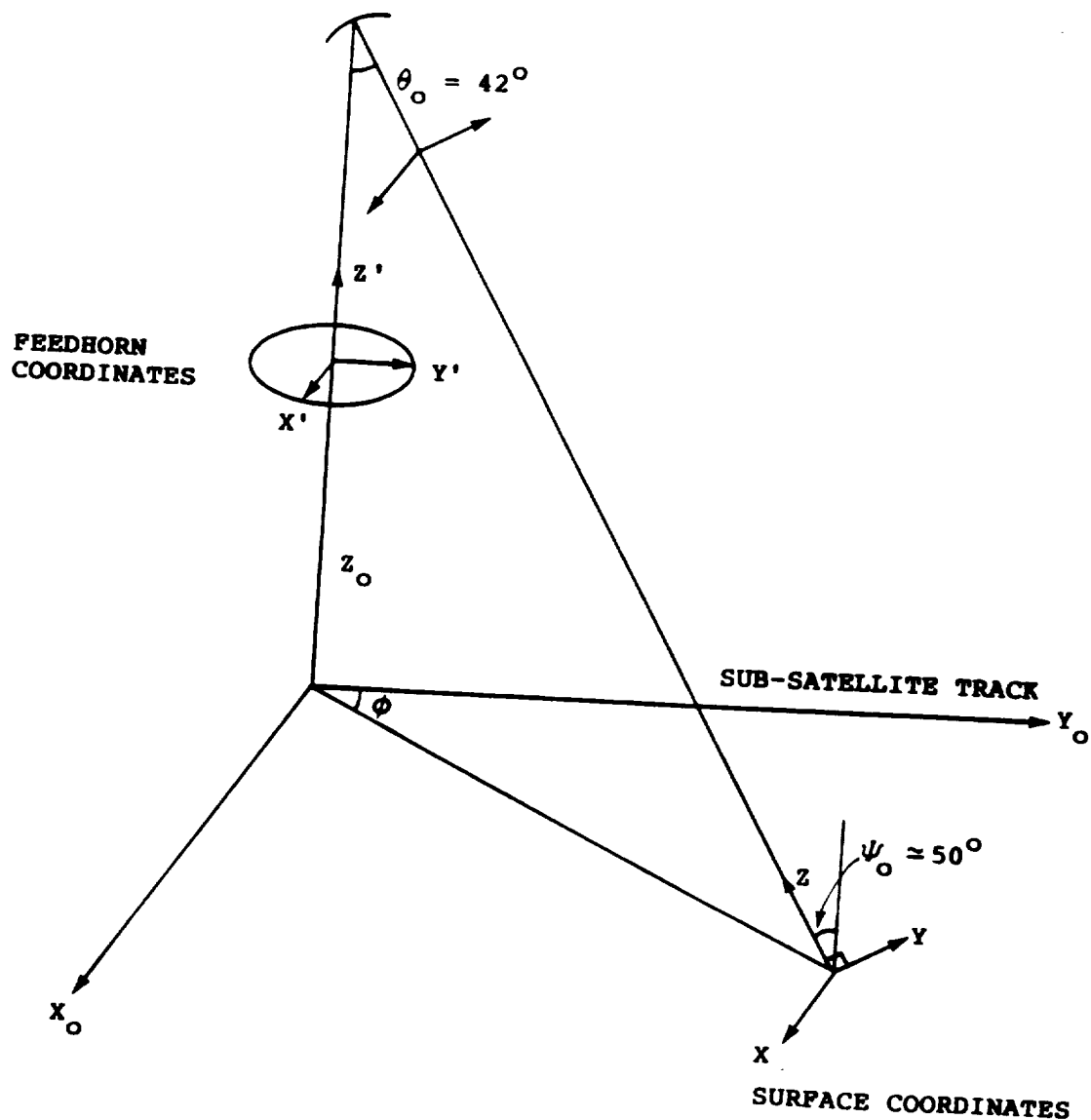FIGURE 4. Input-output relationship for a three-port device.

FIGURE 5. Coordinates of surface and antenna feed horn. The scan
angle φ, as shown, is positive. Also shown are the
antenna look angle θ₀, measured from nadir, and the angle
of incidence at the surface which is about 50°.

$$E_2 = \begin{pmatrix} 1 - k_{1x} & k_{2x}\exp(i\theta_x) \\ k_{2y}\exp(i\theta_y) & 1 - k_{1y} \end{pmatrix} \begin{pmatrix} g_x & 0 \\ 0 & g_y \end{pmatrix} E_1, \qquad (7)$$

where θ_x and θ_y are phase differences and E_1 is given by Eq. (6). The power at the output port of switch p, solely due to surface radiation, is given by

$$T_x = <(Re\ E_{2x})^2>_{t,\Omega}, \qquad (8.a)$$

$$T_y = <(Re\ E_{2y})^2>_{t,\Omega}, \qquad (8.b)$$

where $<>_{t,\Omega}$ denotes the averaging operation over t and Ω. From Eqs. (5) through (8), one obtains

$$T_x = A_x[H\cos^2(\phi+\delta_x) + V\sin^2(\phi+\delta_x)] + B_x(H + V), \qquad (9.a)$$

$$T_y = A_y[H\sin^2(\phi+\delta_y) + V\cos^2(\phi+\delta_y)] + B_y(H + V), \qquad (9.b)$$

where

$$H = E_x^2,$$

$$V = E_y^2,$$

$$A_x = \{[g_x^2(1-k_{1x})^2 + g_y^2k_{2x}^2]^2 - [2g_xg_y(1-k_{1x})k_{2x}\sin\theta_x]^2\}^{1/2},$$

$$B_x = 0.5\ [g_x^2(1-k_{1x})^2 + g_y^2k_{2x}^2 - A_x],$$

$$A_y = \{[g_y^2(1-k_{1y})^2 + g_x^2k_{2y}^2]^2 - [2g_yg_x(1-k_{1y})k_{2y}\sin\theta_y]^2\}^{1/2},$$

$$B_y = 0.5\ [g_y^2(1-k_{1y})^2 + g_x^2k_{2y} - A_y],$$

$$\tan(2\delta_x) = 2g_xg_y(1-k_{1x})k_{2x}\cos\theta_x/[g_x^2(1-k_{1x})^2 - g_y^2k_{2x}^2],$$

$$\tan(2\delta_y) = 2g_yg_x(1-k_{1y})k_{2y}\cos\theta_y/[g_y^2(1-k_{1y})^2 - g_x^2k_{2y}^2].$$

We denote by $T_{A,H}$ and $T_{A,V}$ the powers at port A when switch p selects port H and V, respectively. Then $T_{A,H}$ ($T_{A,V}$) is the sum of T_x (T_y) and $Q_{A,H}$ ($Q_{A,V}$) which are noise powers added incoherently along the respective signal paths from the feed horn to port A:

$$T_{A,H} = T_x + Q_{A,H}, \qquad (10.a)$$

$$T_{A,V} = T_y + Q_{A,V}, \qquad (10.b)$$

where $Q_{A,H}$ and $Q_{A,V}$, computed using Eqs. (3) and (4), are given below:

$$Q_{A,H} = \alpha_{pHA}[\alpha_{awH}(1-\alpha_{ahH})t_{ah} + (1-\alpha_{awH})t_{awH}]$$
$$+ \beta_{pVA}[\alpha_{awV}(1-\alpha_{ahV})t_{ah} + (1-\alpha_{awV})t_{awV}]$$
$$+ (1-\alpha_{pHA})t_h,$$

9

$$Q_{A,v} = \alpha_{pVA}[\alpha_{awV}(1-\alpha_{ahV})t_{ah} + (1-\alpha_{awV})t_{awV}]$$
$$+ \beta_{pHA}[\alpha_{awH}(1-\alpha_{ahH})t_{ah} + (1-\alpha_{awH})t_{awH}]$$
$$+ (1-\alpha_{pVA})t_n,$$

where t_{ah}, t_{awH}, t_{awV}, and t_n are physical temperatures of antenna horn, horizontal wave guide, vertical wave guide, and switch assembly, respectively, and $\alpha_{ahH(V)}$, $\alpha_{awH(V)}$ are transmissivities of the antenna horn and wave guide for the horizontally (vertically) polarized signal path. From Eqs. (9) and (10), one obtains

$$\begin{pmatrix} H \\ V \end{pmatrix} = R \begin{pmatrix} T_{A,H} - Q_{A,H} \\ T_{A,v} - Q_{A,v} \end{pmatrix}, \tag{11}$$

where R, which we may term the generalized polarization rotation matrix, is given by

$$R = \begin{pmatrix} A_x \cos^2(\phi+\delta_x) + B_x & A_x \sin^2(\phi+\delta_x) + B_x \\ A_y \sin^2(\phi+\delta_y) + By & A_y \cos^2(\phi+\delta_y) + B_y \end{pmatrix}^{-1} \tag{12}$$

Equation (11), which expresses the surface brightness in terms of the powers at port A for two antenna paths, is one of our two basic sets of calibration equations.

In the remainder of this section, we derive the second basic set of equations. The power at port K of switch c is given by

$$T_K = \alpha_{cw}[\alpha_{ch}T_c + (1-\alpha_{ch})t_{ch}] + (1-\alpha_{cw})t_{cw}, \tag{13}$$

where α_{ch} and α_{cw} are the transmissivities of the cold horn and wave guide, respectively, and t_{ch} and t_{cw} are the physical temperatures of the cold horn and wave guide, respectively.

We denote by $T_{I,H}$, $T_{I,v}$, $T_{I,c}$, $T_{I,w}$ the powers at port I for the four distinct signal paths designated by H, V, C, and W, each of which is defined by a set of swich settings of switches c, p, and s as follows:

    Path H - Switch settings; p on H, c on L, s on A
    Path V - Switch settings; p on V, c on L, s on A
    Path C - Switch settings; p on H, c on K, s on C
    Path W - Switch settings; p on V, c on L, s on C

Applying the input-output relationship of Eq. (4) to each switch along a chosen path, one obtains

$$T_{I,H} = \alpha_{sAI}T_{A,H} + \beta_{sCI}(t_n+\beta_{cKC}T_K) + (1-\alpha_{sAI})t_n, \tag{14}$$

$$T_{I,v} = \alpha_{sAI}T_{A,v} + \beta_{sCI}(t_n+\beta_{cKC}T_K) + (1-\alpha_{sAI})t_n, \tag{15}$$

$$T_{I,c} = \alpha_{sCI}(\alpha_{cKC}T_K + \beta_{cLC}t_n + (1-\alpha_{cKC})t_n)$$
$$+ \beta_{sAI}T_{A,H} + (1-\alpha_{sCI})t_n, \tag{16}$$

10

$$T_{I,w} = \alpha_{sCI}(t_h + \beta_{cKC}T_K) + \beta_{sAI}T_{A,v}$$
$$+ (1-\alpha_{sCI})t_h. \tag{17}$$

The integrate and dump output of the radiometer, denoted by C, is given in terms of the input power, T_I at port I, as follows:

$$C = G(T_I - t_h) + O, \tag{18}$$

where G is the radiometer gain and O an offset added to make C increase with T_I. Both G and O are assumed to remain constant from one end of scan to the other, and are effectively eliminated from calibration equations through introduction of normalized counts, N_H and N_v defined below:

$$N_H \equiv (C_{A,H} - C_w)/(C_C - C_w), \tag{19.a}$$

$$N_v \equiv (C_{A,v} - C_w)/(C_C - C_w), \tag{19.b}$$

where $C_{A,H}$, $C_{A,v}$, C_C, and C_w are the radiometer outputs corresponding to the four paths H, V, C, and W, respectively. Substituting Eq. (18) into Eqs. (19.a) and (19.b), one obtains

$$N_H = (T_{I,H} - T_{I,w})/(T_{I,c} - T_{I,w}), \tag{20.a}$$

$$N_v = (T_{I,v} - T_{I,w})/(T_{I,c} - T_{I,w}). \tag{20.b}$$

Substituting Eqs (14) through (17) into Eqs. (20.a) and (20.b), we obtain the second basic set of calibration equations given below:

$$T_{A,H} = \{[-(\alpha_{sAI} - \beta_{sAI})D - \beta_{sAI}C]N_H$$
$$+ \beta_{sAI}(C-D)N_v + \alpha_{sAI}C\}/\Gamma, \tag{21.a}$$

$$T_{A,v} = \{(-\alpha_{sAI}D + \beta_{sAI}C)N_v - (\beta_{sAI}C)N_H$$
$$+ \alpha_{sAI}C\}/\Gamma, \tag{21.b}$$

where

$$C = (\alpha_{sCI} - \beta_{sCI})\beta_{cKC}T_K + (\alpha_{sAI} - \beta_{sCI})t_h,$$

$$D = -\alpha_{sCI}(\alpha_{cKC} - \beta_{cKC})T_K + \alpha_{sCI}(\alpha_{cKC} - \beta_{cLC})t_h,$$

$$\Gamma = (\alpha_{sAI} - \beta_{sAI})[\alpha_{sAI} + \beta_{sAI}(N_v - N_H)].$$

Using measured quantities, N_H and N_v, one can compute from Eq. (21), $T_{A,H}$ and $T_{A,v}$, and then substitute them into Eq. (11) to obtain surface radiances. Thus, Eqs. (11) and (21) constitute a new set of calibration equations for the Nimbus-7 SMMR.

2.2 37 GHz channels

A schematic diagram of the RF components of a 37 GHz radiometer is shown in Fig. 6. The polarization selector switch shown in Fig. 2 is absent in Fig. 6 because a separate radiometer is utilized for measuring each of two orthogonally polarized radiances. Thus

polarization mixing is solely due to the rotation of the reflector relative to the fixed MFFH. The reasoning of the previous subsection may be adapted here to derive the calibration equations for the 37 GHz channels.

Setting k_{1x}, k_{1y}, k_{2x}, k_{2y} to zero, one obtains from Eq. (9) the following:

$$T_x = A_x (H \cos^2\phi + V \sin^2\phi), \qquad\qquad (22.a)$$

$$T_y = A_y (H \sin^2\phi + V \cos^2\phi), \qquad\qquad (22.b)$$

where

$$A_x = g_x^2,$$

$$A_y = g_y^2.$$

We denote by T_H the power at the input port A of the cal/sig switch (see Fig. 6). Similarly for T_V. Then T_H (T_V) is, as before, the sum of T_x (T_y) and Q_H (Q_V):

$$T_H = T_x + Q_H, \qquad\qquad (23.a)$$

$$T_V = T_y + Q_V, \qquad\qquad (23.b)$$

where Q_H and Q_V are obtained from $Q_{A,H}$ and $Q_{A,V}$ of previous subsection by setting $\alpha_{pHA} = \alpha_{pVA} = 1$, and $\beta_{pVA} = \beta_{pHA} = 0$:

$$Q_H = \alpha_{awH}(1-\alpha_{ahH})t_{ah} + (1-\alpha_{awH})t_{awH},$$

$$Q_V = \alpha_{awV}(1-\alpha_{ahV})t_{ah} + (1-\alpha_{awV})t_{awV},$$

where the symbols have the same meanings as in the previous subsection.

From Eqs.(22) and (23), one obtains

$$\begin{pmatrix} H \\ V \end{pmatrix} = R_{37} \begin{pmatrix} T_H - Q_H \\ T_V - Q_V \end{pmatrix}, \qquad\qquad (24)$$

where R_{37} is gotten from Eq. (12) by setting $\delta_x = \delta_y = 0$, and $B_x = B_y = 0$:

$$R_{37} = \begin{pmatrix} A_x \cos^2\phi & A_x \sin^2\phi \\ A_y \sin^2\phi & A_y \cos^2\phi \end{pmatrix}^{-1} \qquad\qquad (25)$$

In deriving second basic set of equations, we focus our attention on the horizontal radiometer only; the corresponding set of equations for the vertical polarization radiometer will have the same form as that for the horizontal counterpart. The power at port K of swtich c, denoted by T_{1k}, is given by

12

COLD HORN

c, SKY/AMBIENT
SWITCH

K   L

WAVEGUIDE

AMBIENT
TEMP LOAD

REFLECTOR

REFERENCE
TEMP LOAD

C   I

A

R

S

ISOLATOR

MIXER

IF

DETECTOR
CORRELATOR
INTEGRATOR
A/D CONVERTER

s, CAL/SIG
SWITCH

ANTENNA
HORN

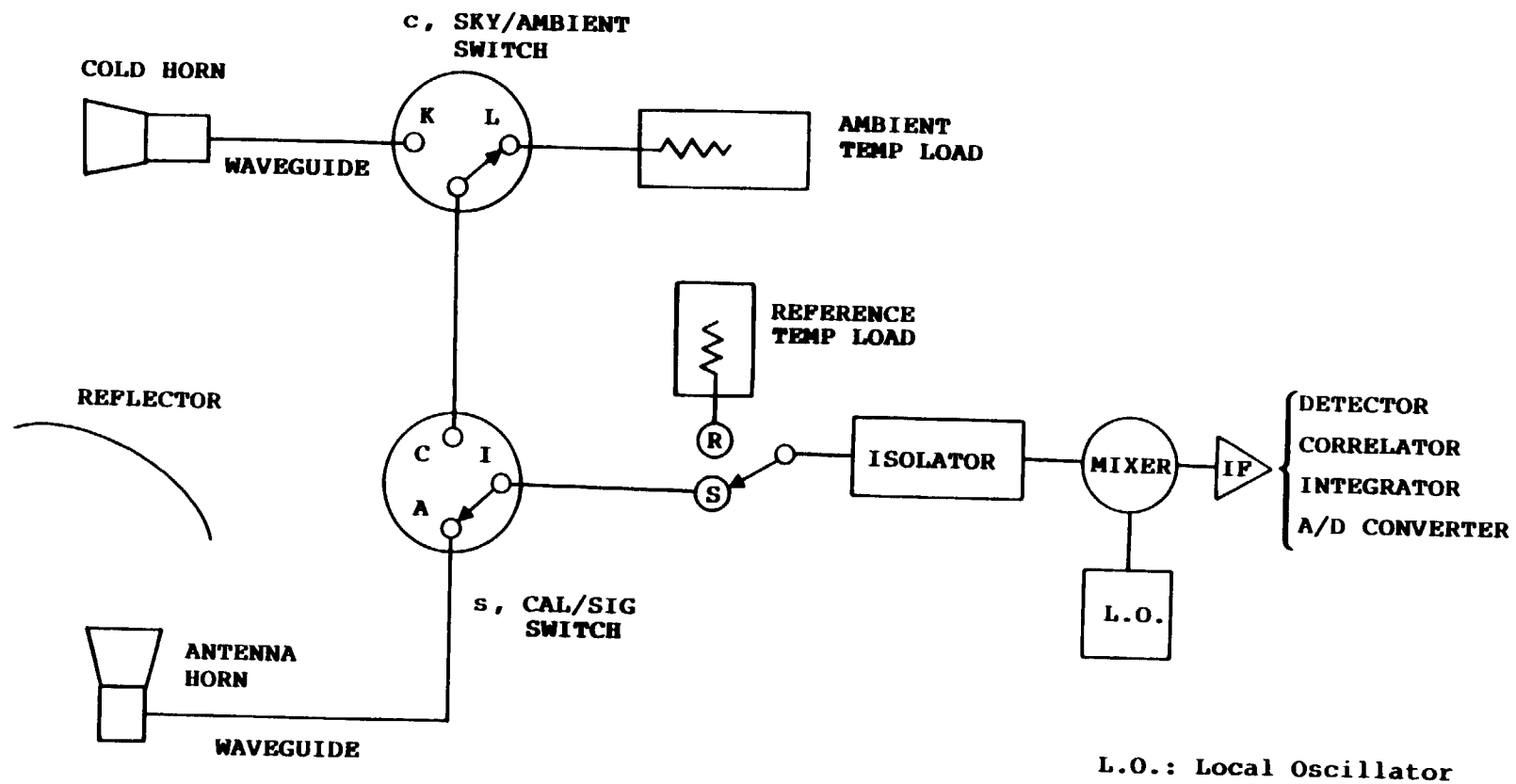L.O.

WAVEGUIDE

L.O.: Local Oscillator

FIGURE 6.   Schematic diagram of the RF components of Nimbus-7 SMMR
- 37 GHz channels.

$$T_{1K} = \alpha_{1cw}[\alpha_{ch}T_c + (1-\alpha_{ch})t_{ch}] + (1-\alpha_{1cw})t_{1cw}, \qquad (26)$$

where α_{ch} and α_{1cw} are the transmissivities of the cold horn and the waveguide, respectively, and t_{ch} and t_{1cw} are the physical temperatures of the cold horn and the waveguide, respectively. The subscripts preceded by 1 (or 2) refer to the variables for the H (or V) polarization radiometers, respectively.

We define $T_{I,H}$, $T_{I,c}$, and $T_{I,w}$ as follows:

$T_{I,H}$ - the power at port I, when s selects A and c selects L;
$T_{I,c}$ - the power at port I, when s selects C and c selects K;
$T_{I,w}$ - the power at port I, when s selects C and c selects L.

Then applying the input-output relationship of Eq. (4) to each switch for a chosen configuration, one obtains

$$T_{I,H} = \alpha_{1sAI}T_H + \beta_{1scI}(t_{1h}+\beta_{1cKc}T_{1K}) \\ + (1-\alpha_{1sAI})t_{1h}, \qquad (27)$$

$$T_{I,c} = \alpha_{1scI}[\alpha_{1cKc}T_{1K} + \beta_{1cLc}t_{1h} + (1-\alpha_{1cKc})t_{1h}] \\ + \beta_{1sAI}T_H + (1-\alpha_{1scI})t_{1h}, \qquad (28)$$

$$T_{I,w} = \alpha_{1scI}(t_{1h} +\beta_{1cKc}T_{1K}) + \beta_{1sAI}T_H \\ + (1-\alpha_{1scI})t_{1h}. \qquad (29)$$

Defining the normalized count, N_H in a manner similar to Eq. (19.a), and applying Eq. (18), one obtains

$$N_H = (T_{I,H} - T_{I,w})/(T_{I,c} - T_{I,w}), \qquad (30)$$

Substituting Eqs. (27) through ((29) into Eq. (30), on obtains

$$T_H = A_H + B_H N_H, \qquad (31)$$

where

$$A_H = (\alpha_{1sAI} - \beta_{1scI})(t_{1h} + \beta_{1cKc}T_{1K})/\Gamma_H,$$

$$B_H = \alpha_{1scI}[(\alpha_{1cKc} - \beta_{1cLc})t_{2h} - (\alpha_{1cKc} - \beta_{1cKc})T_{1K}]/\Gamma_H,$$

$$\Gamma_H = \alpha_{1sAI} - \beta_{1sAI}.$$

Similarly for the 37 GHz vertical polarization radiometer, one obtains

$$T_V = A_V + B_V N_V, \qquad (32)$$

where

$$A_V = (\alpha_{2sAI} - \beta_{2scI})(t_{2h} + \beta_{2cKc}T_{2K})/\Gamma_V,$$

$$B_V = \alpha_{2scI}[(\alpha_{2cKc} - \beta_{2cLc})t_{2h} - (\alpha_{2cKc} - \beta_{2cKc})T_{2K}]/\Gamma_V,$$

14

$$\Gamma_v = \alpha_{2\bullet AI} - \beta_{2\bullet AI}.$$

Eqs. (24), (31), and (32) constitute the basic calibration equations for the 37 GHz radiometers of the new model - substituting Eqs. (31) and (32) into Eq. (24), we get a relationship that expresses surface radiances in terms of measured quantities.

3.0 CURRENT CALIBRATION EQUATIONS

The calibration equations currently in use for for the Nimbus-7 SMMR data production can be derived from the results of Section 2 if we reinstate the assumption that switch leakages are negligible. In this section we will derive current calibration equations for only those that utilize polarization selector switches since the derivation of the calibration equations for the 37 GHz radiometers is rather straightforward.

Setting all the leakage factors appearing in Eqs. (21.a) and (21.b) to zero, we obtain simplified expressions for $T_{A,H}$ and $T_{A,v}$:

$$T_{A,H} = t_h + \alpha_0(T_K - t_h)N_H, \tag{33.a}$$

$$T_{A,v} = t_h + \alpha_0(T_K - t_h)N_v, \tag{33.b}$$

where $\alpha_0 = \alpha_{\bullet cI}\alpha_{cKc}/\alpha_{\bullet AI}$, and T_K is given by Eq. (13).

Polarization rotation, which accounts for not only the antenna scan but also the polarization mixing at switch p, is effected empirically by introducing "offset angles", δ_x and δ_y into the polarization rotation matrix given below:

$$R' = \begin{pmatrix} \cos^2(\phi+\delta_x) & \sin^2(\phi+\delta_x) \\ \sin^2(\phi+\delta_y) & \cos^2(\phi+\delta_y) \end{pmatrix}^{-1} \tag{34}$$

The matrix, R', when compared with R (Eq. (12)), is seen to account for the effect of switch leakages (in switch p) only partially in that the factors A_x and A_y and biases B_x and B_y in R are not present in R'. Replacing R of Eq. (11) by R' and substituting into it $T_{A,H}$ and $T_{A,v}$ of Eqs. (33.a) and (33.b), we obtain the current calibration equations given below:

$$\begin{pmatrix} H \\ V \end{pmatrix} = R' \begin{pmatrix} t_h - Q'_{A,H} + \alpha_0(T_K - t_h)N_H \\ t_h - Q'_{A,v} + \alpha_0(T_K - t_h)N_v \end{pmatrix}, \tag{35}$$

where $Q'_{A,H}$ and $Q'_{A,v}$ proceed from $Q_{A,H}$ and $Q_{A,v}$ by setting β_{pVA} and β_{pHA} to zero.

4.0 FURTHER DISCUSSION

A new calibration scheme for the Nimbus-7 SMMR is studied in this report. The apparent deviation of the measured radiances from the anticipated symmetry in scan angle is explained by this model

through including leakages at the polarization selector switch. This feature, asymmetry in scan angle, is caused by the interference between horizontally and vertically polarized fields which, having traveled different paths and merging at the polarization selector switch, have path differences comparable with the wavelengths of the microwave radiation.

Another important aspect of the new calibration model is that it offers a possibility of deriving "absolutely calibrated" radiances, which are necessary to test and validate models for surface and atmosphere. It is clear from Eqs. (11) and (21) that the values of transmissivities and leakage factors must be known prior to implementing the new model in the SMMR data processing. Only a few transmissivities had been determined before launch, and none of leakage factors have been measured on the assembled instrument. Attempts to determine some leakage factors using in-flight data were unsuccessful because of the difficulties of estimating the surface brightness, H and V of Eq. (11), to the accuracy required for such an analysis. Without means of obtaining acceptable values of α's and β's, it appears impossible to derive absolutely calibrated brightness temperatures from in-flght measurements alone. However, if ground measurements are made, which are colocated in space and time with the SMMR measurements, and a good atmospheric model is available, then it is possible to achieve absolute calibration.

In the absence of the desired ground measurements, the new calibration equations can still be useful in understanding the evolutionary nature of the aging instrument's problems. Instead of attempting to determine α's and β's, we start with a set of preassigned values of α's and β's and compute from measured quantities, N_H and N_V, the surface brightness temperatures in accordance with Eqs. (11) and (21). The new brightness temperatures can be scrutinized whether their long-term behavior is satisfactory or not, or may be used to derive geophysical parameters whose validity can be tested against ground measurements. If comparisons show that the new brightness temperatures produce better results than the current ones, we may adopt the presumed values of α's and β's as representing the instrument's status. In this manner, we may identify and assess the cause(s) of some of the instrument's problems.

REFERENCES

Gloersen, P., 1983: Calibration of the Nimbus-7 SMMR: II Polarization mixing corrections, TM 84976, NASA/Goddard Space Flight Center, Greenbelt, Maryland.

Gloersen, P., and F. T. Barath, 1977: A scanning multichannel microwave radiometer for Nimbus-G and SeaSat-A, IEEE J. Oceanic Eng., OE-2, 172-178

Gloersen, P., D. J. Cavalieri, and H. V. Soule, 1980: An alternate algorithm for correction of the scanning multichannel microwave

radiometer polarization radiances using Nimbus-7 observed data, TM 80672, NASA/Goddard Space Flight Center, Greenbelt, Maryland.

Report Documentation Page

1. Report No. NASA TM	2. Government Accession No.	3. Recipient's Catalog No.

4. Title and Subtitle Effects of Switch Leakages Upon Nimbus-7 SMMR Calibration	5. Report Date June 1988
	6. Performing Organization Code 636

7. Author(s) Daesoo Han and Seung T. Kim	8. Performing Organization Report No.
	10. Work Unit No. 665-10-70

9. Performing Organization Name and Address Goddard Space Flight Center Greenbelt, MD 20771	11. Contract or Grant No. NAS5-29386
	13. Type of Report and Period Covered Technical Memorandum

12. Sponsoring Agency Name and Address National Aeronautics and Space Administration Washington, DC 20546	14. Sponsoring Agency Code

15. Supplementary Notes

Daesoo Han: Goddard Space Flight Center
Seung T. Kim: ST Systems Corporation

16. Abstract

A calibration model for the Nimbus-7 Scanning Multichannel Microwave Radiometer (SMMR) is studied. This model not only removes major drawbacks of the current calibration model but also helps us understand the performance degradation of the aging instrument. The current Nimbus-7 SMMR calibration algorithm was derived without considering the interference effect between the two orthogonally polarized signals merging at a ferrite polarization selector switch. The resulting calibrated brightness temperatures, considered as a function of scan angle ϕ, are not symmetric around $\phi = 0$. However, neither the origin of the asymmetry nor the manner in which the two orthogonal components are mixed has been fully understood.

The new calibration model proposed in this paper incorporates all the leakage factors associated with the ferrite switches along the signal paths. The resulting calibration equations clarify how the orthogonal components of surface brightness are coupled at radiometers. As a consequence, the origin of the asymmetry is clearly identified and explained. In addition, the feasibility of "absolute calibration" using in-orbit data is discussed.

17. Key Words (Suggested by Author(s)) Scanning Multichannel Microwave Radiometer, Calibration, Switch Leakage	18. Distribution Statement Unclassified -- Unlimited Subject Category 18

19. Security Classif. (of this report) Unclassified	20. Security Classif. (of this page) Unclassified	21. No. of pages 17	22. Price